Partial Volume Correction of Doubly-Gated Cardiac Datasets using Anatomical and Edge-Preserving Priors.

A. Turco[1], J.Duchenne[2], O. Gheysens[1,3], J. Nuyts[1], J.U. Voigt[2,4], P. Claus[2], K. Vunckx[1]

I. Introduction

Positron emission tomography (PET) images suffer from partial volume (PV) effects due to the poor spatial resolution of the PET system. In cardiac imaging, additional blurring is caused by the breathing motion and the beating of the heart. Dual gating of the cardiac datasets is one possible approach to remove the motion blur [1], but it dramatically reduces the statistics of the dataset and leads to extremely noisy reconstructions (still to be corrected for PV).

A way to improve the noise characteristics and deal with PV effect is represented by anatomy-based PV correction (PVC) during PET reconstruction. The use of such technique has shown promising results in brain [2], but its extension to cardiac datasets needs further validation. Particularly, several concerns linked to the use of anatomical information arise, including more cumbersome and time-consuming acquisition and processing, and being prone to gating discrepancies and mis-registration issues. As an alternative, edge-preserving and de-noising techniques have also been presented in the past [3], [4], promising noise reduction and edge preservation without the use of any anatomical side information.

Our first aim is to verify whether the application of anatomy-based PVC on doubly-gated cardiac PET datasets is feasible and whether the correct PET quantification is hampered if anatomy and emission image are misaligned, due to an incorrect choice of the phase of the high-resolution CT (HRCT) or to mis-registration. Secondly, we evaluate the use of two edge-preserving priors and compare the resulting images to the anatomy-based PVC-reconstructions and to the standard ordered-subsets expectation maximization (OSEM3D) reconstructions.

II. Methods

XCAT simulation study: Simulated results were generated with the help of the XCAT phantom [5]. One static image of the thorax was produced, with the heart captured in a fixed cardiac and respiratory phase. This procedure simulates a cardiac ^{18}F-FDG PET scan where the cardiac and respiratory gating have ideally removed all motion present in the dataset. The tissues were filled with realistic activity values obtained from a real measured dataset (see Fig. 1). Two lesions, non-transmural (L1) and transmural (L2), were also added to the left ventricle (LV) of the heart. A corresponding attenuation image was generated with the XCAT software and used both for attenuation and for anatomical information (HRCT1). Before being used as anatomical prior, HRCT1 was converted to Hounsfield units (HU) and underwent contrast enhancement of the blood pools.

In addition, the simulated anatomical image was shifted by 2 mm both in the x and in the z direction, with the aim of verifying the robustness of the anatomy-based prior to mis-registration. These shift values are realistic [6] and especially likely to occur when noisy emission datasets are considered. This shifted anatomical image was converted to HU and contrast-enhanced (HRCT2), and used as alternative anatomical information during reconstruction. Furthermore, a second XCAT attenuation image was generated in the same respiratory phase and in the next cardiac gate compared to the emission image (assuming a cardiac cycle divided in 10 gates), to simulate a difference in the gating of the PET and the HRCT datasets. Converted to HU and contrast-enhanced, it was used as a third anatomical prior (HRCT3) during the reconstruction of the initial cardiac PET gate. Noise-free sinograms were generated. Attenuation and a shift-invariant camera resolution were modelled, but scatter and randoms were not. In addition, Poisson noise was added to each sinogram to simulate a realistic, doubly-gated acquisition (effective time/frame = 36s). Twenty-five noise realizations were simulated.

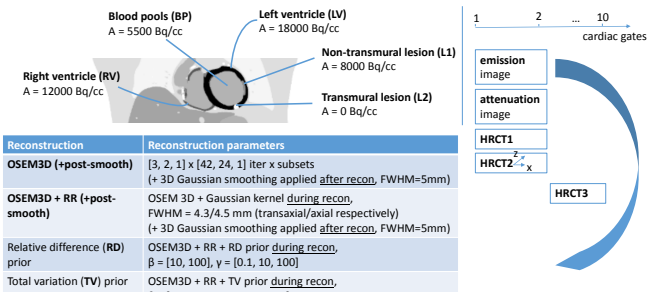

Reconstruction	Reconstruction parameters
OSEM3D (+post-smooth)	[3, 2, 1] x [42, 24, 1] iter x subsets (+ 3D Gaussian smoothing applied after recon, FWHM=5mm)
OSEM3D + RR (+post-smooth)	OSEM 3D + Gaussian kernel during recon, FWHM = 4.3/4.5 mm (transaxial/axial respectively) (+ 3D Gaussian smoothing applied after recon, FWHM=5mm)
Relative difference (**RD**) prior	OSEM3D + RR + RD prior during recon, β = [10, 100], γ = [0.1, 10, 100]
Total variation (**TV**) prior	OSEM3D + RR + TV prior during recon, β = [0.0001, 0.001, 0.01, 0.1], i = 5
Bowsher - perf (HRCT1)	OSEM3D + RR + Asymmetrical Bowsher with RD β = [0.1, 4, 10], γ = 0 n = [6, 9, 13] spherical neighbourhood (3x3x3)
Bowsher – shift (HRCT2)	
Bowsher – mism (HRCT3)	

Fig. 1. Overview of the simulation study and of the performed reconstructions.

Reconstructions: Each of the sinograms was reconstructed using OSEM3D, with and without resolution recovery (RR). The resulting OSEM3D images were either used as such, or post-smoothed with a Gaussian kernel of 5 mm (FWHM) in all directions. These reconstructions were compared to the reconstructions regularized with the relative difference (RD) [7] and the total variation (TV) [8] prior. Also, reconstructions using the asymmetrical Bowsher prior [9] were included in

[1] KU Leuven - University of Leuven, Department of Imaging and Pathology, Nuclear Medicine and Molecular imaging, Medical Imaging Research Center (MIRC), B-3000 Leuven, Belgium.[2] KU Leuven - University of Leuven, Department of Cardiovascular Sciences, Cardiology, Medical Imaging Research Center (MIRC), B-3000 Leuven, Belgium. [3] University Hospitals Leuven, Department of Nuclear Medicine, B-3000 Leuven, Belgium. [4] University Hospitals Leuven, Department of Cardiovascular Diseases, B-3000 Leuven, Belgium.

This work is supported by KU Leuven OT/12/084 and Research Foundation - Flanders (FWO)

the comparison, using the matching and the two mismatched anatomical images. Attenuation correction was performed during reconstruction, based on the well-aligned attenuation image. The PET reconstruction voxel size was 1.35^3 mm^3. A [3, 2, 2] x [42, 24, 1] (iterations x subsets) iteration scheme was used to reconstruct all Hirez datasets.

Different parameter sets were tested for each of the reconstructions with priors (see Fig. 1). For each prior, we tested different weights (β). In addition, the Bowsher prior operates locally. A spherical neighbourhood of 18 voxels was chosen. Moreover, a fixed number of neighbours (n) within the neighbourhood needs to be set, to define over which voxels the smoothing is applied. The TV prior is an iterative regularization method, thus a certain number of iterations (i) has to be imposed too. An overview of all the parameters used during reconstruction is in Fig. 1. The results here presented focus on a selection of all the reconstructions performed. The selection was performed based on a visual comparison of the resulting images in terms of sharpness of the anatomies and noise reduction. Particularly, the chosen Bowsher reconstructions use a weight (β) of 10, γ = 0, and 13 neighbours were selected out of the 18-neighbours spherical neighbourhood. The reconstructions with the RD prior are performed using β =10 and γ = 10, whereas the TV prior has β = 0.01 and 5 internal iterations.

Image analysis: Three figures of merit were used to evaluate the performances of the different reconstruction algorithms:

- The recovery coefficient (RC) was chosen to describe the behaviour of the different algorithms in terms of over- or under- estimation of the reconstructed activity, if compared to the true activity. The RC is defined as follows:

$$RC_r = \frac{\bar{r}^{recon}}{\bar{r}^{true}}, r = LV, RV, L1$$

  where $\bar{r}$ represents taking the mean in the volume of interest r, and LV, RV and L1 are the volumes of interest containing the left ventricle, the right ventricle and the non-transmural lesion, respectively (see Fig. 1). The RC was not calculated for L2, as its true mean value is zero.

- The contrast recovery coefficient (CRC) was used to identify the algorithm that best preserves the contrast between the region of interest r and the background region b, if compared to the ground truth represented by the original phantom. The CRC was computed as in [10]:

$$CRC_r = \frac{contrast_r^{recon}}{contrast_r^{true}}, r = LV, RV, L1, L2$$

  where

$$contrast_r = \frac{\bar{r}}{\bar{b}} - 1,$$

$$b = \begin{cases} BP & \text{if r = LV, RV} \\ LV & \text{if r = L1, L2} \end{cases}$$

  BP and L2 are volumes of interest containing the blood pool and the transmural lesion, respectively (see Fig. 1).

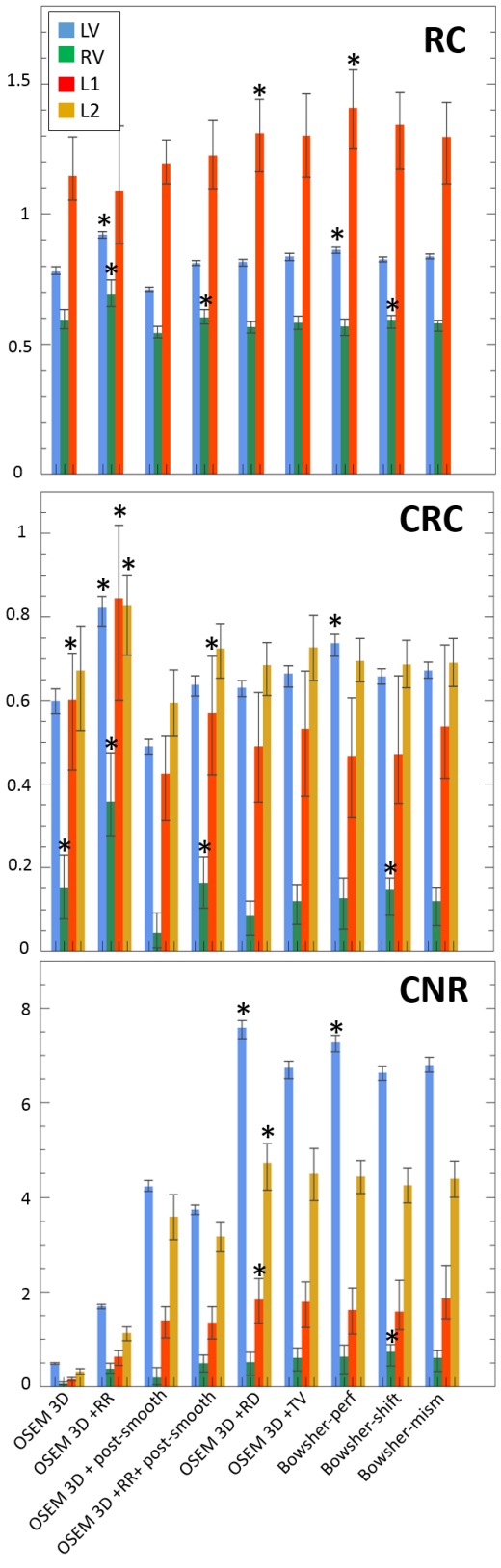

Fig. 2. Figures of merit for the different heart regions. Top pane: recovery coefficient (RC). Middle pane: contrast recovery coefficient (CRC). Bottom pane: contrast-to-noise ratio (CNR). The asterisk (*) indicates the cases where the algorithm scores significantly *better* than the TV (p=0.01).

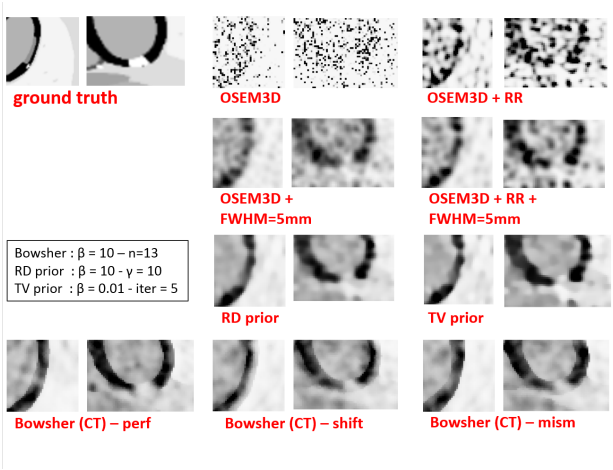

Fig. 3. Zoomed in images of the lesions, reconstructed with the different algorithms.

- The contrast to noise ratio (CNR) is another common measure for determining the performance of an algorithm. In fact, due to the noise present in the final image, the CRC alone does not imply better detectability of the anatomies or lesions. This figure of merit is particularly important in the context of lesion detection. The CNR was defined as in [11]:

$$CNR_r = \frac{contrast_r^{recon}}{noise_b^{recon}}, r = LV, RV, L1, L2$$

where

$$noise_b = \frac{\overline{stddev(b)}}{\bar{b}},$$

$$b = \begin{cases} BP & \text{if r = LV, RV} \\ LV & \text{if r = L1, L2} \end{cases}$$

$\overline{stddev(b)}$ is obtained by calculating the standard deviation on the activity in every voxel in b over all noise realizations and then taking the average over all voxels in b.

III. Results

In the simulated noisy datasets, the best recovery of the average activity values is obtained with the OSEM3D+RR algorithm alone. However, its high noise coupled with the Gibbs artefacts produced by the RR makes it extremely hard to clearly distinguish the anatomies, as Fig. 3 shows. The addition of gaussian post-smoothing improves the visual appearance of such reconstruction, at the price of a decreased CRC.

The images reconstructed with the edge-preserving priors are more homogeneous within distinct regions and have better noise properties than the un-regularized OSEM3D+RR with and without post-smoothing.

The CNR increases for all regularized reconstructions, if compared to the CNR that a bare post-smoothing can achieve. However, all priors fail to correctly delineate the RV and the L1 lesion, which at times appears smaller and almost transmural. Due to the absence of lesions in the anatomical image used, the Bowsher prior tends to smooth over the edges of the lesions, thus overestimating their mean value.

When the shifted anatomical image is used, the L2 lesion decreases in size and the wall becomes artificially thin. Additionally, artefactual hypo-perfused areas appear (see LV of Figure 3, Bowsher(CT) - shift).

IV. Discussion and Conclusions

The results of this study show a slight superiority of the anatomy-based prior in terms of contrast recovery of the ventricles and volume delineation, provided that the anatomical information is well aligned to the corresponding emission image. There is no improvement in terms of lesion detection, if compared to e.g. the TV prior. In fact, the anatomical image here simulated does not show any intensity difference between lesions and healthy tissue – which nevertheless corresponds to a realistic scenario, as in a CT image the difference between infarcted tissue and healthy tissue is often not detectable. The edge-preserving priors, on the other hand, produce visually appealing images too, with better CNR if compared to the current standard for PET reconstruction (OSEM + post-smoothing), thus suggesting better lesion detectability. In addition, they have the advantage of not relying on an external, additional scan for anatomy, which might be shifted or mismatched and therefore useless or even deleterious for myocardial quantification and lesion detection.

The use of a different imaging modality as anatomical information, able to better highlight the underlying scar tissue (e.g. MRI), is currently being simulated and evaluated. This is expected to yield better results, particularly in the case where anatomy and emission are perfectly aligned.

References

[1] S.G. Nekolla, J. Dinges, and C. Rischpler. Clinical impact of cardiac-gated PET imaging. *PET Clinics*, 8(1):69–79, 2013.

[2] K. Vunckx, P. Dupont, K. Goffin, W. Van Paesschen, K. Van Laere, and J. Nuyts. Voxel-based comparison of state-of-the-art reconstruction algorithms for 18F-FDG PET brain imaging using simulated and clinical data. *Neuroimage*, 102 Pt 2:875–884, Nov 2014.

[3] A. Buades, B. Coll, and J. M. Morel. A review of image denoising algorithms, with a new one. *Multiscale Model Simul*, 4(2):490–530, 2005.

[4] M Burger, J Mller, E Papoutsellis, and C B Schnlieb. Total variation regularization in measurement and image space for pet reconstruction. *Inverse Problems*, 30(10):105003, 2014.

[5] W. P. Segars, G. Sturgeon, S. Mendonca, J. Grimes, and BM. Tsui. 4D XCAT phantom for multimodality imaging research. *Med Phys*, 37(9):4902:15, 2010.

[6] F. Maes, A. Collignon, D. Vandermeulen, G. Marchal, and P. Suetens. Multimodality image registration by maximization of mutual information. *IEEE Trans Med Imaging*, 16(2):187–198, Apr 1997.

[7] J. Nuyts, D. Beque, P. Dupont, and L. Mortelmans. A concave prior penalizing relative differences for maximum-a-posteriori reconstruction in emission tomography. *IEEE Trans Nucl Sci*, 49:56–60, 2002.

[8] A. Chambolle and T. Pock. A first-order primal-dual algorithm for convex problems with applications to imaging. *Journal of Mathematical Imaging and Vision*, 40(1):120–145, 2011.

[9] K. Vunckx and J. Nuyts. Heuristic modification of an anatomical markov prior improves its performance. In *IEEE Nucl Sci Symp Conf Rec*, pages 3262–3266, Oct 2010.

[10] Ching-Han Hsu. A study of lesion contrast recovery for iterative PET image reconstructions versus filtered backprojection using an anthropomorphic thoracic phantom. *Computerized Medical Imaging and Graphics*, 26(2):119 – 127, 2002.

[11] D. Dickerscheid, J. Lavalaye, L. Romijn, and J. Habraken. Contrast-noise-ratio (CNR) analysis and optimisation of breast-specific gamma imaging (BSGI) acquisition protocols. *EJNMMI Res*, 3(1):21, 2013.